

Supporting Information for

Electrochemical treatment of human waste coupled with

molecular hydrogen production

Kangwoo Cho, Daejung Kwon and Michael R. Hoffmann

Experimental Details	2
Kinetic Model Derivation	5
Figure Captions	9
Fig. S1 – S7	11
References	18

Experimental

Materials. NaCl and concentrated sulfuric acid were used as received from Macron Chemicals. Crystalline phenol (99.6%) and Na₂C₂O₄ were purchased from J.T. Baker. Total Protein Reagent, Folin-Ciocalteu's phenol reagent, protein standard (bovin serum albumin), TiOSO₄, H₂IrCl₆, [O₂CCH₂C(OH)(CO₂)CH₂CO₂]Bi, Bi₂O₃, SnCl₄, and TaCl₅ were received from Sigma Aldrich. Chemical oxygen demand (COD) digestion solution, COD standard solution (potassium acid phthalate), total nitrogen (TN) reagent set, DPD total chlorine reagent powder, chlorine standard solution were received from Hach. Jack Bean Urease was provided by the Worthington Biochemical Corporation. All other chemicals were supplied by Mallinckrodt. Ti metal sheet (Ti-Gr.2 sheet, 0.50 mm thick) was purchased from ThyssenKrupp Materials. All electrolyte and standard solutions were prepared in MilliQ water (18.2 MO cm) from a Millipore Milli-Q gradient water purification system.

BiO_x/TiO₂ electrode preparation. A Ti metal sheet (0.5 mm thick) was sand-blasted with SiC paper (120 – 240 grits) and degreased with acetone. The precursor solution for the anti-passivation layer was prepared as 73 mM H₂IrCl₆ with 27 mM TaCl₅ in 4 M HCl solution. Both sides of pretreated Ti support were brushed by the precursor and annealed at 525 °C for an hour. This procedure was repeated for 5 times with the same annealing temperature for 10 minutes duration. A sealing coat was deposited twice by painting 225 mM SnCl₄ and 12.5 mM Bi₂O₃ in 0.5 M HCl solution and baking at 425 °C for 10 minutes. Precipitates from dissolving 10 mmol Bi₂O₃ and 0.48 mol TiOSO₄ in 1.2 M Na₂CO₃ (1 L) were calcined at 830 °C for 45 minutes to

produce bismuth oxide doped titanium dioxide ($\text{BiO}_x/\text{TiO}_2$) nanoparticles. The precursor for the $\text{BiO}_x/\text{TiO}_2$ thin film (overcoat solution) was 160 mM $\text{Ti}(\text{OCH}_2\text{CH}_2\text{O})_2$ (i.e., the preparation details are described in elsewhere) with 80 mM $[\text{O}_2\text{CCH}_2\text{C}(\text{OH})(\text{CO}_2)\text{CH}_2\text{CO}_2]\text{Bi}$ in a 0.24 M NH_4OH solution. To prepare the slurry deposition layer, $\text{BiO}_x/\text{TiO}_2$ particles dispersed in MilliQ water (3 M metal concentration) were brushed on air dried; after this step a 25-fold diluted overcoat solution was sequentially pasted on to the surface. The slurry deposit was baked on at 250 for 5 minutes; this procedure was repeated for 7 times. In the final sequence, a thin film of $\text{BiO}_x/\text{TiO}_2$ deposit was made by repetitive sealing with overcoat solution annealed at 250 °C (4 times) and then at 450 °C (2 times).

Electrochemical methods. Before all electrochemical experiments, the electrodes were rinsed with acetone and large amount of MilliQ water. The electrode module was allowed to equilibrate with the electrolyte solution in an open circuit for 1 hr while monitoring the open circuit potential of anode and cathode. As a routine procedure, the pH, conductivity and the ohmic resistance between anode and reference electrode (R) were measured before and after the electrochemical experiments. The R was measured by current interruption method with current bias of 100 mA. For the chrono-voltammetric data collection, the current intensity (J) was averaged from 400 to 500 seconds. The variation of current density after 500 seconds was not significant, since the p-values of paired t-test between averaged current from 400 to 500 seconds and from 500 to 1800 seconds were always larger than 0.05.

Model septic tank effluent preparation. The COD degradation during the anaerobic incubation

followed an exponential decay trend, where initial decomposition of macro-molecules was followed by mineralization of organics with exponential growth of microorganisms, initially presented in domestic wastewater (DWW). Urea was hydrolyzed to give ammonium ion enzymatically using urease; this resulted in an increase of the pH of the model septic tank effluents (STEs) up to 9. The increase in pH resulted in a considerable amount of precipitation of minerals including magnesium ammonium phosphate (struvite). The supernatant of the collected DWW and prepared STEs was used in the experiments to minimize the effects of particulate matters.

Analyses. COD was measured with standard digestion kits with a low detection range (3 – 150 mg L⁻¹); the kits were prepared in order to eliminate the interference of the ammonium ion in the COD analysis¹ by controlling the kinetics for ammonium and COD oxidation steps separately. Samples were diluted to adjust the chloride concentration far below the interference range (2,000 mg L⁻¹) as suggested by the digestion kit supplier (Hach, USA). For the Dionex DX-500 Ion Chromatography (IC) system, hypochlorite appeared to have a peak at a retention time identical to the chloride ion with superimposable calibration curves. Since the hypochlorite would be detected both in the IC analysis and total chlorine (Cl_{DPPD}) analysis, the sum of [Cl⁻], [Cl_{DPPD}] and [ClO₃⁻] exceeded the initial chloride concentration, particularly for the electrolysis in pure NaCl solution. In this case, [Cl⁻] was calibrated by subtracting the difference which corresponds to [ClO₃⁻]. For urea measurement, 5 mL of diluted samples in 15 mL conical tubes were added by 2 mL of urease solution (63.1 mg L⁻¹) and incubated in water bath (50 °C) for 20 min. Treated samples were cooled down in room temperature (RT) for IC analysis. Urea measurements were

performed only for the intact electrolyte before the electrolysis due to the interference of free chlorine. In phenol-sulfuric acid method,² 0.4 mL samples in glass tubes were mixed with 0.4 mL phenol solution (5 W/V%) and 2 mL sulfuric acids (95%) to measure the absorbance at 470 nm after reaction for 30 min at RT. For protein measurement,³ 0.5 mL samples were introduced to 2.5 mL total protein reagent in 15 mL conical tubes with gentle inversion for several times. After reaction for 10 min at RT, twofold diluted Folin-Ciocalteu's phenol reagent of 0.2 mL was added with vigorous mixing. With further holding at RT for 30 min, the absorbance of the supernatant was measured at 600 nm. NH₄Cl, NaOCl, NaClO₃, NaNO₂, NaNO₃, HCOONa, Na₂C₂O₄, CH₃COONa, MgSO₄ and CaCl₂ were used as standards with proper concentration range for the IC analysis. Potassium acid phthalate, NH₄Cl, chlorine, bovine serum albumin and glucose solution were used as a standard for COD, TN, Cl_{DPD}, protein and carbohydrate analysis, respectively.

Kinetic Model Derivation

Kinetic equations in the absence of oxidizable pollutants.

$$\frac{d[MO_x(ClO^-)]}{dt} = k_{4a}[MO_{x+1}][Cl^-] - k_{4b}[MO_x(ClO^-)][Cl^-][H^+]^2 = 0 \quad (S1)$$

$$\frac{d[Cl^-]}{dt} = -k_{4a}[MO_{x+1}][Cl^-] - k_{4b}[MO_x(ClO^-)][Cl^-][H^+]^2 + k_{5a}[Cl_2] - k_{-5a}[HOCl][Cl^-][H^+] \quad (S2)$$

$$\frac{d[Cl_2]}{dt} = k_{4a}[MO_{x+1}][Cl^-] - k_{5a}[Cl_2] + k_{-5a}[HOCl][Cl^-][H^+] = 0 \quad (S3)$$

$$\frac{d[HOCl]}{dt} = k_{5a}[Cl_2] + k_{-5a}[HOCl][Cl^-][H^+] - k_{5b}[HOCl] + k_{-5b}[ClO^-][H^+] - k_{6b}[MO_{x+1}]^2[HOCl] \quad (S4)$$

$$\frac{d[\text{ClO}^-]}{dt} = k_{5b}[\text{HOCl}] - k_{-5b}[\text{ClO}^-][\text{H}^+] - k_{6a}[\text{MO}_{x+1}]^2[\text{ClO}^-] \quad (\text{S5})$$

$$\frac{d[\text{ClO}_3^-]}{dt} = k_{6a}[\text{MO}_{x+1}]^2[\text{ClO}^-] + k_{6b}[\text{MO}_{x+1}]^2[\text{HOCl}] \quad (\text{S6})$$

Eq. S1 implies a pseudo-steady-state assumption for the surface bound ClO^- , while Eq. S3 is based on the negligible amount of Cl_2 at circum-neutral pH. Assuming that active sites are saturated at high current densities (quasi-constant $[\text{MO}_{x+1}]$), we use Eq. S1 and Eq. S3 in Eq. S2 to obtain

$$\frac{d[\text{Cl}^-]}{dt} = -k_{4a}[\text{MO}_{x+1}][\text{Cl}^-] = -k_4^{\text{eff}}[\text{Cl}^-] \quad (7)$$

By denoting $[\text{FC}] = [\text{Cl}_2] + [\text{HOCl}] + [\text{ClO}^-]$, Eq. S3-S5 gives

$$\frac{d[\text{FC}]}{dt} = k_{4a}[\text{MO}_{x+1}][\text{Cl}^-] - k_{6a}[\text{MO}_{x+1}]^2[\text{FC}] = k_4^{\text{eff}}[\text{Cl}^-] - k_6^{\text{eff}}[\text{FC}] \quad (8)$$

Assuming that k_{6a} is comparable to k_{6b} and $[\text{FC}] \sim [\text{HOCl}] + [\text{ClO}^-]$ at circum-neutral pH,

$$\frac{d[\text{ClO}_3^-]}{dt} = k_{6a}[\text{MO}_{x+1}]^2[\text{FC}] = k_6^{\text{eff}}[\text{FC}] \quad (9)$$

Instantaneous Current Efficiency (ICE) for free chlorine (FC) and chlorate without the presence of organics. Substituting the analytical solutions of Eq. 7 – 9 to Eq. 10 yields,

$$ICE_{\text{FC}} = \frac{2[k_4^{\text{eff}} \exp(-k_4^{\text{eff}}t) - \frac{k_4^{\text{eff}}k_6^{\text{eff}}}{k_6^{\text{eff}} - k_4^{\text{eff}}} \{\exp(-k_4^{\text{eff}}t) - \exp(-k_6^{\text{eff}}t)\}]}{\frac{2k_3^{\text{eff}}}{[\text{Cl}^-]_0} + 2k_4^{\text{eff}} \exp(-k_4^{\text{eff}}t) + \frac{4k_4^{\text{eff}}k_6^{\text{eff}}}{k_6^{\text{eff}} - k_4^{\text{eff}}} \{\exp(-k_4^{\text{eff}}t) - \exp(-k_6^{\text{eff}}t)\}} \quad (\text{S8})$$

Where, $[\text{Cl}^-]_0$ denotes the initial chloride concentration.

$$\text{When } t \rightarrow 0, ICE_{FC} = \frac{k_4^{eff}}{\frac{k_3^{eff}}{[Cl^-]_0} + k_4^{eff}} \quad (S9)$$

Similarly, the instantaneous current efficiency for chlorate formation is expressed as

$$ICE_{ClO_3^-} = \frac{\frac{6k_4^{eff}k_6^{eff}}{k_6^{eff}-k_4^{eff}}\{\exp(-k_4^{eff}t)-\exp(-k_6^{eff}t)\}}{\frac{2k_3^{eff}}{[Cl^-]_0}+2k_4^{eff}\exp(-k_4^{eff}t)+\frac{4k_4^{eff}k_6^{eff}}{k_6^{eff}-k_4^{eff}}\{\exp(-k_4^{eff}t)-\exp(-k_6^{eff}t)\}} \quad (S10)$$

Kinetic equations in the presence of pollutants. The governing equations for chloride and FC with the presence of pollutants are derived by modifying Eq. 7 and 8 as:

$$\frac{d[Cl^-]}{dt} = -k_4^{eff}[Cl^-] + k_{13}[FC][COD] + (3k_{14} + 4k_{15})[FC][NH_4^+] \quad (S11)$$

$$\frac{d[FC]}{dt} = k_4^{eff}[Cl^-] - k_6^{eff}[FC] - k_{13}[FC][COD] - (3k_{14} + 4k_{15})[FC][NH_4^+] \quad (16)$$

By treating the FC mass balance analyses for the bulk-phase and the electrode boundary layer separately, we employ pseudo-steady-state approximations for the FC to give

$$\frac{d[FC]_{SS}^A}{dt} = k_4^{eff}[Cl^-] - k_6^{eff}[FC]_{SS}^A - \frac{k_m^{FC}}{\delta}([FC]_{SS}^A - [FC]_{SS}^B) = 0 \quad (S12)$$

$$\frac{d[FC]_{SS}^B}{dt} = \frac{k_m^{FC}}{\delta}([FC]_{SS}^A - [FC]_{SS}^B) - [FC]_{SS}^B\{k_{13}[COD] + (3k_{14} + 4k_{15})[NH_4^+]\} = 0 \quad (S13)$$

Where, $[FC]_{SS}^A$ and $[FC]_{SS}^B$ are quasi-steady-state FC concentration in the anode vicinity and in bulk, k_m^{FC} is the mass transfer coefficient for the FC and δ is the depth of boundary layer. Since $[FC]_{SS}^A \gg [FC]_{SS}^B$, the solutions of Eq. S12 and S13 are reduced to

$$[FC]_{SS}^A = \frac{k_4^{eff}[Cl^-]}{k_6^{eff} + k_m^{FC}/\delta} \equiv C_{[FC]_{SS}^A} [Cl^-] \quad (S14)$$

$$[FC]_{SS}^B = \frac{\left(k_m^{FC}/\delta\right)k_4^{eff}[Cl^-]}{\left(k_6^{eff} + k_m^{FC}/\delta\right)(k_{13}[COD] + (3k_{14} + 4k_{15})[NH_4^+])} \equiv \frac{C_{[FC]_{SS}^B} [Cl^-]}{(k_{13}[COD] + (3k_{14} + 4k_{15})[NH_4^+])} \quad (S15)$$

Also, the mass balance equation for chloride (Eq. S11) and chlorate (Eq. 9) are modified as

$$\frac{d[Cl^-]}{dt} = -k_4^{eff}[Cl^-] + k_{13}[FC]_{SS}^B[COD] + (3k_{14} + 4k_{15})[FC]_{SS}^B[NH_4^+] \quad (S16)$$

$$\frac{d[ClO_3^-]}{dt} = k_6^{eff}[FC]_{SS}^A \quad (S17)$$

Instantaneous Current Efficiency (ICE) for COD degradation. Substituting Eq. S14 and S15

into Eqs. 21 – 24 gives

$$ICE_{COD} = \frac{4C_{[FC]_{SS}^B}}{\left(\frac{2k_3^{eff}}{[Cl^-]} + 2k_4^{eff} + 4C_{[FC]_{SS}^A} k_6^{eff}\right) \left(1 + \frac{(3k_{14} + 4k_{15})[NH_4^+]}{k_{13}[COD]}\right)} \quad (S18)$$

$$ICE_{N_2} = \frac{4C_{[FC]_{SS}^B}}{\left(\frac{2k_3^{eff}}{[Cl^-]} + 2k_4^{eff} + 4C_{[FC]_{SS}^A} k_6^{eff}\right) \left(1 + \frac{4k_{15}}{3k_{14}} + \frac{k_{13}[COD]}{3k_{14}[NH_4^+]}\right)} \quad (S19)$$

$$ICE_{NO_3^-} = \frac{4C_{[FC]_{SS}^B}}{\left(\frac{2k_3^{eff}}{[Cl^-]} + 2k_4^{eff} + 4C_{[FC]_{SS}^A} k_6^{eff}\right) \left(1 + \frac{3k_{14}}{4k_{15}} + \frac{k_{13}[COD]}{4k_{15}[NH_4^+]}\right)} \quad (S20)$$

$$ICE_{ClO_3^-} = \frac{6C_{[FC]_{SS}^A} k_6^{eff}}{\frac{2k_3^{eff}}{[Cl^-]} + 2k_4^{eff} + 4C_{[FC]_{SS}^A} k_6^{eff}} \quad (S21)$$

Figure Captions

Fig. S1. Dependence of (a) IR compensated anodic potential ($E_a - IR$) on applied anodic potential (E_a), (b) cell potential ($E_a - E_c$) on E_a and (c) logarithmic current density (J) on the $E_a - IR$ during chronovoltammetric experiment in a single compartment electrolysis cell with 10 mM (square, $R = 21.9 \Omega$), 30 mM (triangle, $R = 6.8 \Omega$) and 50 mM (circle, $R = 4.8 \Omega$) NaCl solution (275 mL).

Fig. S2. (a) Evolution of the formate concentration and (b) current variation under sequential substitution (2 mL, arrows) with 10 mM NaCOOH (σ : 0.92 mS/cm) in a potentiostatic (E_a : 3 V), single compartment electrolysis cell; Initial electrolyte: 5.3 mM KH_2PO_4 47.5 mL (pH: 7.2, σ : 0.92 mS/cm).

Fig. S3. Evolution of (a) chlorine species, (b) organic species, (c) nitrogen species, and (b inlet) cations (Ca^{2+} , Mg^{2+}) concentration in a potentiostatic (E_a : 3 V) WEC experiment (J : $247 \pm 6 \text{ A m}^{-2}$, $E_a - iR$: $2.15 \pm 0.02 \text{ V}$, $E_a - E_c$: $5.41 \pm 0.04 \text{ V}$) with diluted human urine (pH: 6.6, σ : 6.05 mS/cm, 55 mL).

Fig. S4. Evolution of (a) current density (J), (b) IR -compensated anodic potential ($E_a - IR$), and (c) cell voltage ($E_a - E_c$) in potentiostatic (E_a : 3 V) WEC experiment with model septic tank effluents; STE1 (green), STE2 (blue), STE3 (red), STE4 (black). Each inset figure shows the mean value with standard deviation in error bar.

Fig. S5. Scatter plot for (a) protein, (b) carbohydrate, and (c) carboxylates concentration versus COD concentration together with (a, inlet) pseudo-first-order rate constants for protein degradation in potentiostatic (E_a : 3 V) WEC experiments with model septic tank effluents; STE1 (circle), STE2 (square), STE3 (triangle), STE4 (diamond). Arrows indicate an arbitrary varying direction along with time.

Fig. S6. Variations in (a) COD concentration, (b) TN concentration, (c) nitrate concentration, and (d) chlorate concentration as a function of specific passed charge in potentiostatic (E_a : 3 V) WEC experiments with model septic tank effluents; STE1 (circle), STE2 (square), STE3 (triangle), STE4 (diamond).

Fig. S7. (a) Variation in absorbance spectra (270 – 500 nm) along with the electrolysis time and (b) absorbance at 425 nm as a function of electrolysis time in potentiostatic (E_a : 3 V) WEC experiments with STE4. Inset figure in (b) visualizes the color variation.

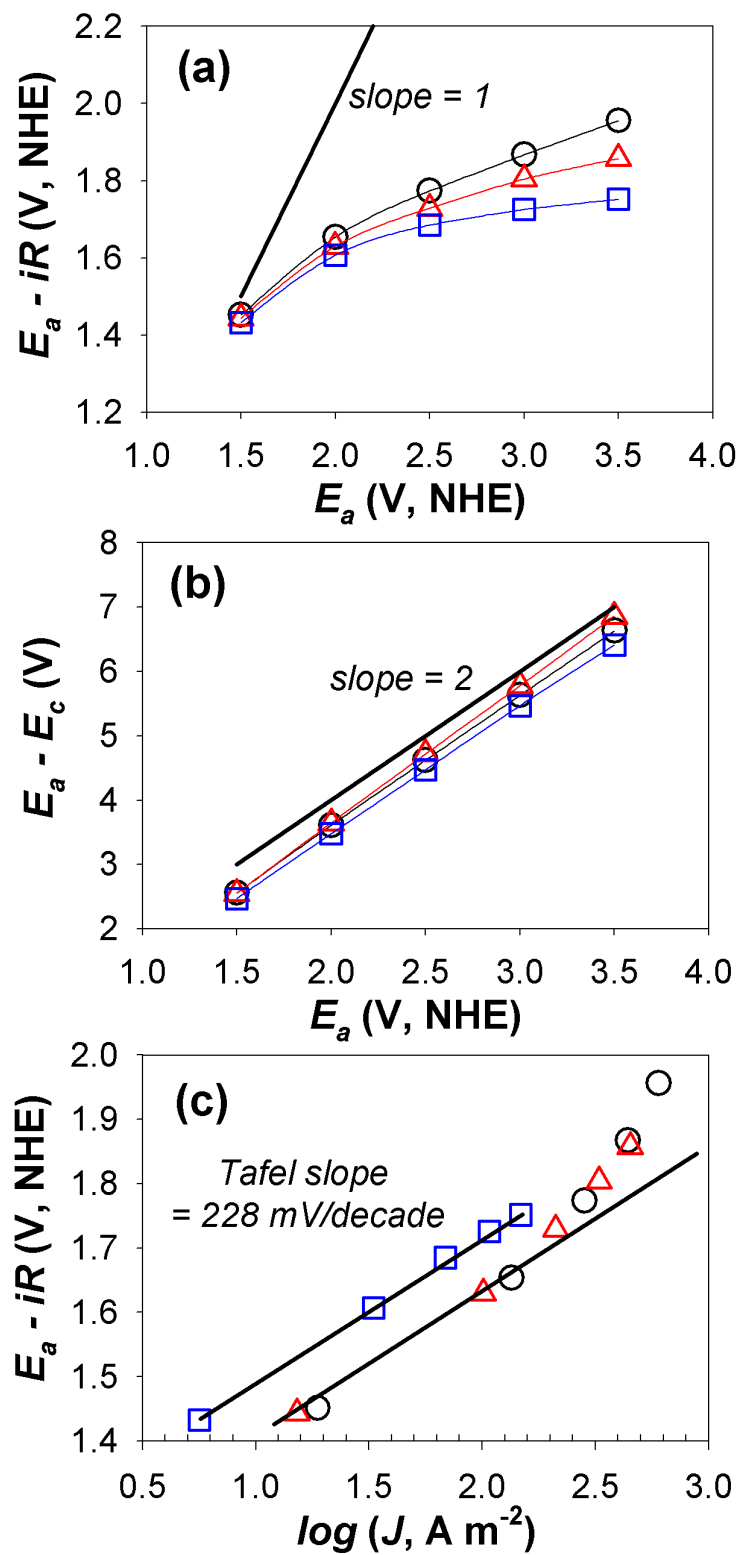


Fig. S1.

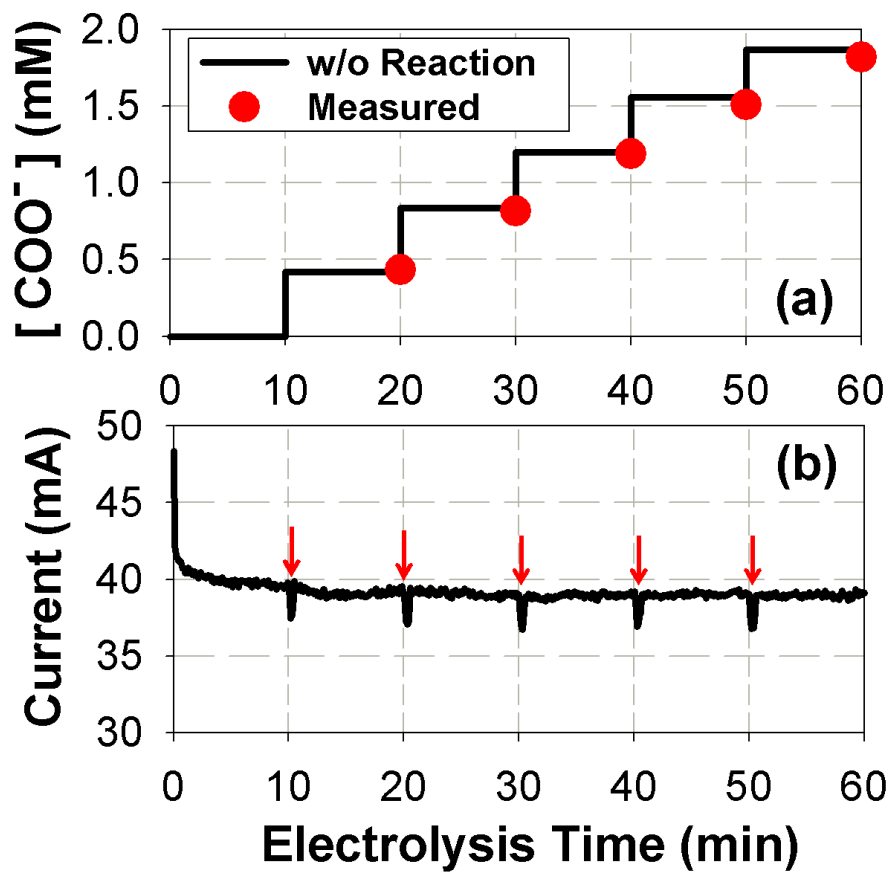


Fig. S2.

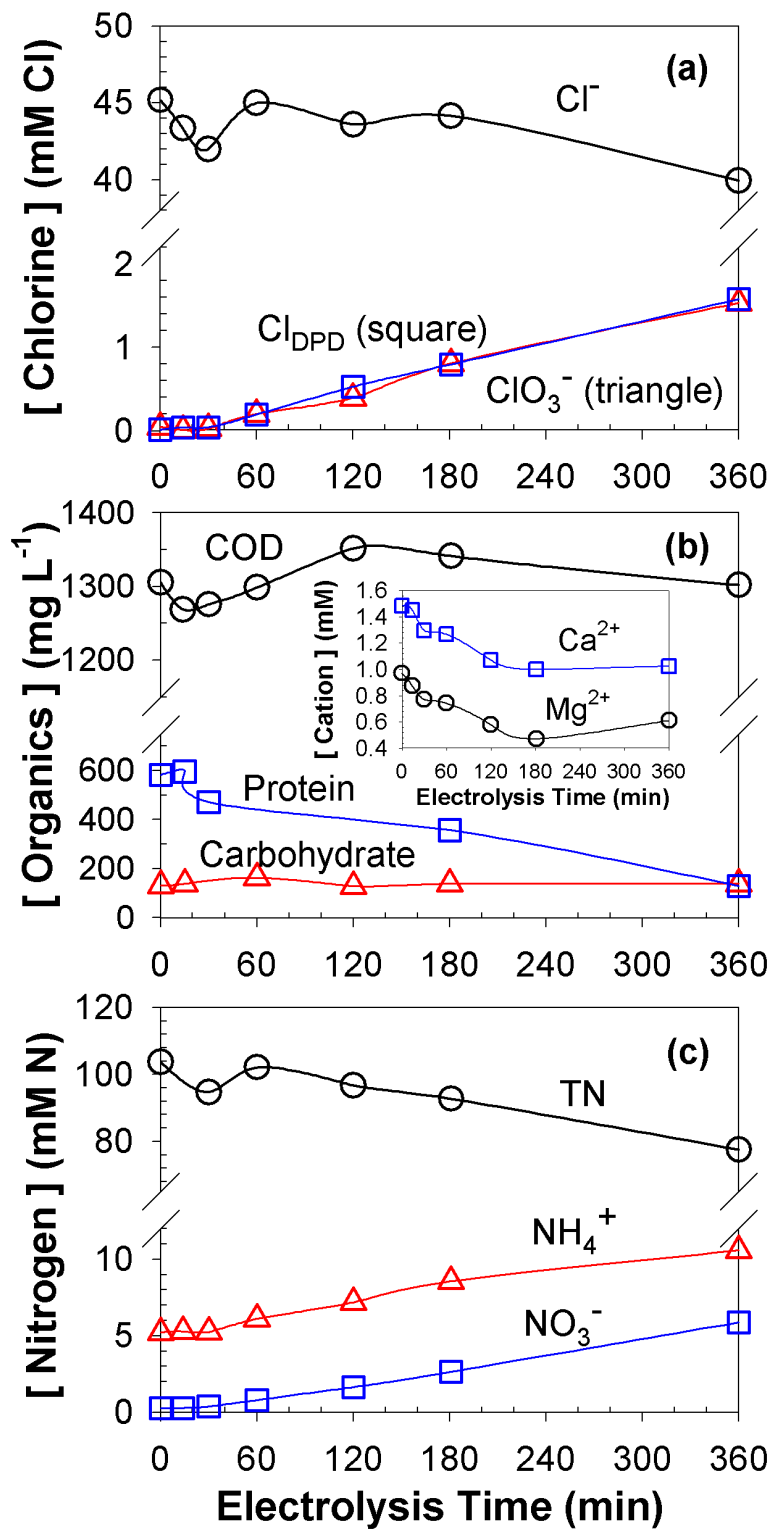


Fig. S3.

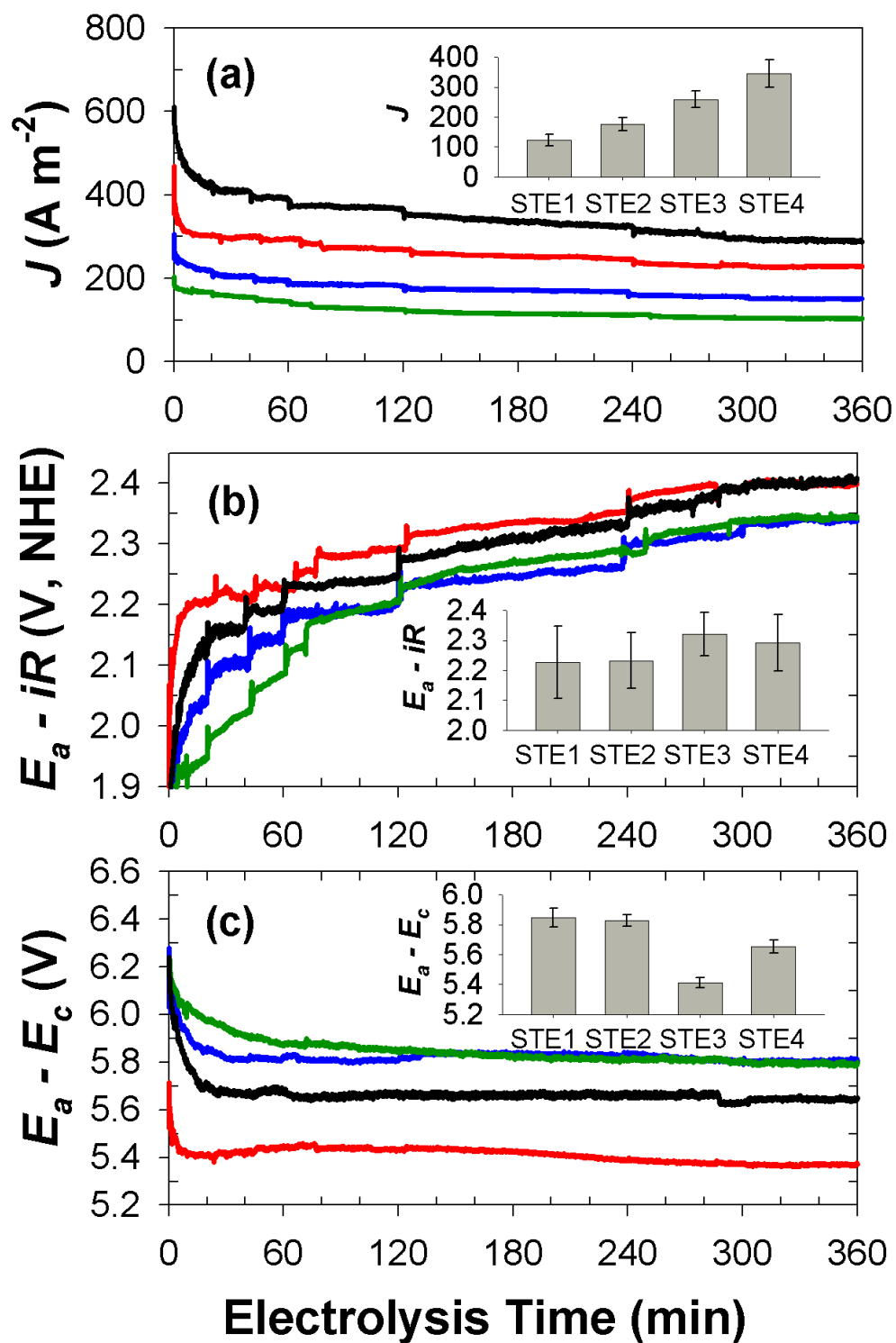


Fig. S4.

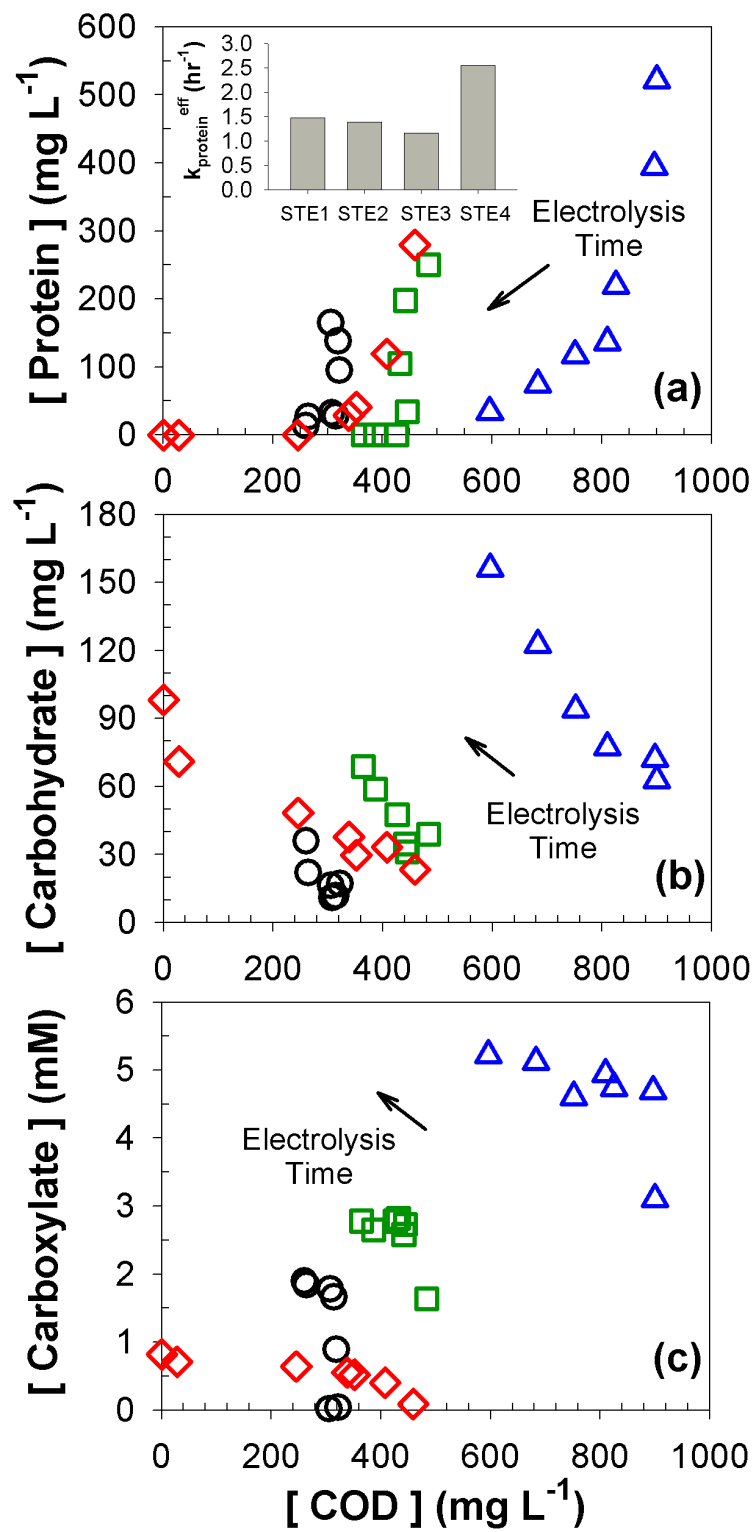


Fig. S5.

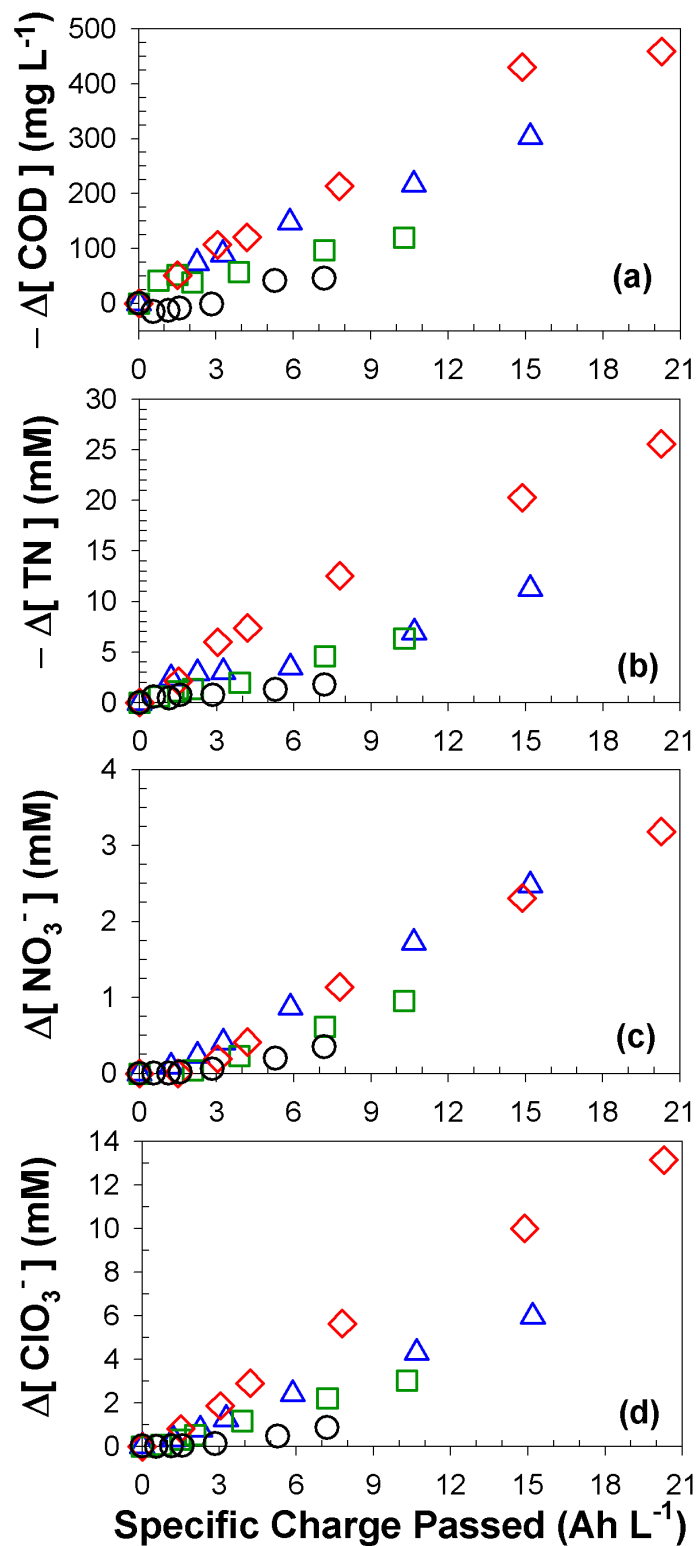


Fig. S6.

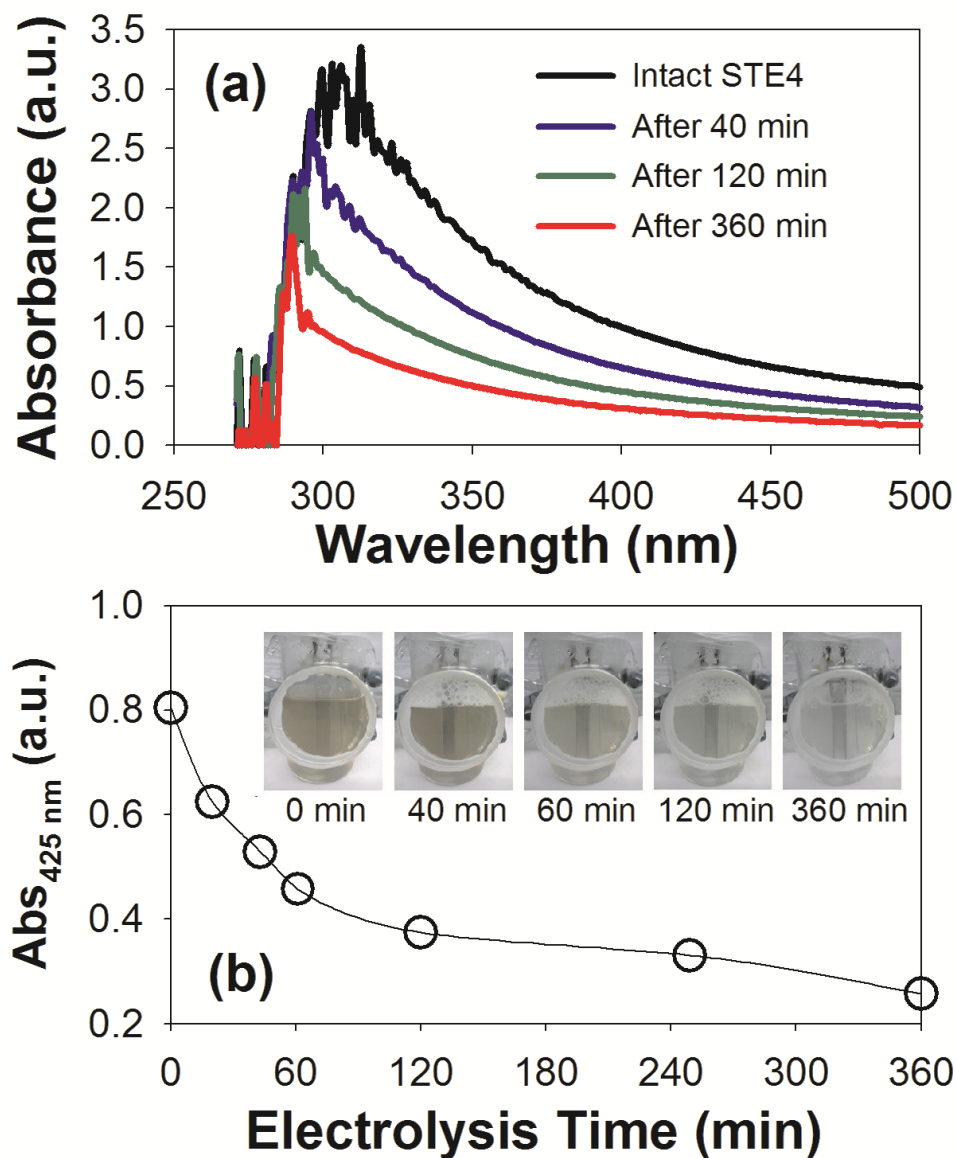


Fig. S7.

References

1. B. R. Kim, *J. Water. Pollut. Conf.*, 1989, **61**, 614-617.
2. M. Dubois, K. A. Gilles, J. K. Hamilton, P. A. Rebers and F. Smith, *Anal. Chem.*, 1956, **28**, 350-356.
3. O. H. Lowry, N. J. Rosebrough, A. L. Farr and R. J. Randall, *J. Biol. Chem.*, 1951, **193**, 265-275.